Anal. Chem. **2006,** *78,* 5474−5479

Multichannel PCR-CE Microdevice for Genetic Analysis

Chung N. Liu,[†] Nicholas M. Toriello,[‡] and Richard A. Mathies*[,‡,§]

Department of Chemical Engineering, UCSF/UC Berkeley Joint Graduate Group in Bioengineering, and Department of Chemistry, University of California, Berkeley, California 94720

We have developed a fully integrated multichannel polymerase chain reaction-capillary electrophoresis (PCR-CE) microdevice with nanoliter reactor volumes for highly parallel genetic analyses. Resistance temperature detectors and heaters made out of Ti/Pt are integrated on the microchip using a scalable radial design to provide precise temperature control of the four parallel PCR-CE reactor systems. Heating rates of >15 °C s^{-1} and cooling rates of >10 °C s^{-1} allow cycle times of 50 s and 30 complete PCR cycles in <27 min. PDMS membrane valves control and localize PCR reagents in the 380-nL reactors. By directly integrating PCR reactors with the CE separation system, efficient coupling of amplification with separation is achieved. The microdevice demonstrates good amplification uniformity and sensitivity down to 10 initial template copies in the 380-nL reactor (~43 aM) with signal-to-noise ratio greater than 10. Parallel PCR-CE multiplex amplification and genetic analyses of four different samples with (1) both *M13mp18* control template and *E. coli* K12 cells, (2) only *M13mp18* template, (3) only *E. coli* K12 cells, and (4) negative control are completed in less than 30 min in a single run.

Miniaturization and integration of conventional analytical protocols on a microdevice, i.e., the so-called micro total analysis system or lab-on-a-chip, have been suggested for nearly a decade to address the inefficiency, high analysis cost, and long analysis time associated with conventional macroscopic analytical techniques.[1,2] Microfabricated devices are attractive because of their ability to integrate multiple complex processes at the nanoliter scale in a highly parallel fashion on a single device, leading to shorter analysis time and lower reagent consumption. Early work on the integration of chemical reactions with analysis on a microchip focused on simple processes such as fluorescence labeling[3] and DNA restriction digestion.[4] Since then, the functional integration of complex processes such as PCR amplification coupled to CE[5] in a microchip has been developed. To achieve higher levels of integration, microdevices incorporating injectors, mixers, heating chambers, and separation channels have also been reported.[6,7] Despite this rapid advancement, a high-throughput parallel multichannel PCR-CE microdevice has yet to be realized.

PCR is an indispensable technique for genetic analysis, but conventional PCR suffers from long assay times due to slow thermal transition rates and high analysis cost due to microliter reaction volumes. To alleviate these problems, an ideal PCR microdevice should allow rapid thermal cycling at low reaction volume and perform sensitive multiplex PCR in a parallel format. One of the first integrated PCR microdevices consisted of a silicon reactor attached to a glass CE channel to amplify and directly analyze and detect PCR products.[8] Microfluidic PCR devices have since been fabricated in different substrates such as silicon,[9−11] glass,[12−15] and silicon−glass hybrids.[16] Glass microfluidic devices are advantageous because glass surfaces can be chemically modified for compatibility with many different assays. Moreover, glass microfluidic devices are easily fabricated with conventional wet etching techniques, have good thermal properties compared to plastic microdevices, have high dielectric strength and low background fluorescence, and are optically transparent in the visible wavelengths used for optical sensing.

A variety of PCR microdevices have been developed with the goal of high-speed and low-volume amplification. In a continuous-

* Corresponding author. Phone: (510) 642-4192. Fax: (510) 642-3599. E-mail: rich@zinc.cchem.berkeley.edu.

[†] Department of Chemical Engineering.

[‡] UCSF/UC Berkeley Joint Graduate Group in Bioengineering.

[§] Department of Chemistry.

(1) Manz, A.; Graber, N.; Widmer, H. M. *Sens. Actuators, B* **1990**, *1*, 244−248.
(2) Harrison, D. J.; Manz, A.; Fan, Z. H.; Ludi, H.; Widmer, H. M. *Anal. Chem.* **1992**, *64*, 1926−1932.
(3) Jacobson, S. C.; Hergenroeder, R.; Moore, A. W. J.; Ramsey, J. M. *Anal. Chem.* **1994**, *66*, 4127−4132.
(4) Jacobson, S. C.; Ramsey, J. M. *Anal. Chem.* **1996**, *68*, 720−723.
(5) Lagally, E. T.; Simpson, P. C.; Mathies, R. A. *Sens. Actuators, B* **2000**, *63*, 138−146.
(6) Burns, M. A.; Mastrangelo, C. H.; Sammarco, T. S.; Man, F. P.; Webster, J. R.; Johnson, B. N.; Foerster, B.; Jones, D.; Fields, Y.; Kaiser, A. R.; Burke, D. T. *Proc. Natl. Acad. Sci. U.S.A.* **1996**, *93*, 5556−5561.
(7) Pal, R.; Yang, M.; Lin, R.; Johnson, B. N.; Srivastava, N.; Razzacki, S. Z.; Chomistek, K. J.; Heldsinger, D. C.; Haque, R. M.; Ugaz, V. M.; Thwar, P. K.; Chen, Z.; Alfano, K.; Yim, M. B.; Krishnan, M.; Fuller, A. O.; Larson, R. G.; Burke, D. T.; Burns, M. A. *Lab Chip* **2005**, *5*, 1024−1032.
(8) Woolley, A. T.; Hadley, D.; Landre, P.; deMello, A. J.; Mathies, R. A.; Northrup, M. A. *Anal. Chem.* **1996**, *68*, 4081−4086.
(9) Wilding, P.; Kricka, L. J.; Cheng, J.; Hvichia, G.; Shoffner, M. A.; Fortina, P. *Anal. Biochem.* **1998**, *257*, 95−100.
(10) Daniel, J. H.; Iqbal, S.; Milington, R. B.; Moore, D. F.; Lowe, C. R.; Leslie, D. L.; Lee, M. A.; Pearce, M. J. *Sens. Actuators, A* **1998**, *71*, 81−88.
(11) Northrup, M. A.; Benett, B.; Hadley, D.; Landre, P.; Lehew, S.; Richards, J.; Stratton, P. *Anal. Chem.* **1998**, *70*, 918−922.
(12) Waters, L. C.; Jacobson, S. C.; Kroutchinina, N.; Khandurina, J.; Foote, R. S.; Ramsey, J. M. *Anal. Chem.* **1998**, *70*, 5172−5176.
(13) Lagally, E. T.; Medintz, I.; Mathies, R. A. *Anal. Chem.* **2001**, *73*, 565−570.
(14) Zhang, N. Y.; Tan, H. D.; Yeung, E. S. *Anal. Chem.* **1999**, *71*, 1138−1145.
(15) Ferrance, J. P.; Wu, Q.; Giordano, B.; Hernandez, C.; Kwok, Y.; Snow, K.; Thibodeau, S.; Landers, J. P. *Anal. Chim. Acta* **2003**, *500*, 223−236.
(16) Cheng, J.; Shoffner, M. A.; Hvichia, G. E.; Kricka, L. J.; Wilding, P. *Nucleic Acids Res.* **1996**, *24*, 380−385.

10.1021/ac060335k CCC: $33.50
Published on Web 07/01/2006

flow PCR chip,[17] sample flowing through serpentine channels with three different temperature zones achieved 20 thermal cycles in 1.5 min, but the PCR yield was low. Since then, Hashimoto et al.[18] and Obeid et al.[19] utilized a similar scheme to complete 20 and 30 PCR cycles in 1.7 and 6 min, respectively. Because the serpentine flow PCR microdevice relies on sample flowing through regions held at different temperatures, these devices are bulky and require high initial copy numbers for successful detection. To obtain low-volume PCR, Koh et al.[20] developed a 29-nL PCR reactor on a poly(cyclic olefin) microdevice with a limit of detection (LOD) of six copies. Even with integrated heaters and temperature sensors this device required 80 min for complete thermal cycling. Parallel PCR systems down to 3 nL have been developed in poly(dimethylsiloxane) (PDMS) microdevices to minimize reagent usage.[21] However, this approach required placing the entire microdevice in a conventional thermal cycler and resulted in 1 h reaction times and reduced sensitivity to ~60 starting copies. A recent review noted that the fastest PCR microdevices tend to use the largest starting template copy number and largest volumes, while the lowest volume PCR microdevices are the slowest.[22]

Our previous work demonstrated rapid and sensitive PCR-CE analysis in a single 280-nL reactor having an integrated heater and a RTD on a glass substrate.[23,24] The goal of this study is to develop an array of integrated PCR-CE systems that are capable of performing multiple PCR-CE analyses in parallel. The challenges in arraying the PCR-CE microchip include developing robust fluidic components for positive control of the PCR reagents during thermal cycling, designing an easily fabricated heater that addresses multiple PCR reactors in parallel without thermal gradients, and optimizing the location of multiple RTD sensors to monitor sample temperature. We present here the development of this multichannel PCR-CE microdevice and evaluate the amplification uniformity, limit of detection, and multiplex analysis capability of the microdevice.

EXPERIMENTAL SECTION

Microdevice Design. A schematic of the four-layer glass/PDMS multichannel PCR-CE microdevice is shown in Figure 1a. Four independently addressable PCR-CE systems are arrayed in a symmetrical doublet format on a 100-mm glass wafer. Each system contains a heater, resistance temperature detector, PDMS microvalves, PCR chamber (380 nL), and coupled CE separation channel (5-cm effective length) for parallel PCR amplification and size-based separation of PCR amplicons. The two reactors within a doublet share common cathode and waste reservoirs, while the two doublets share a common anode reservoir. The reactor region

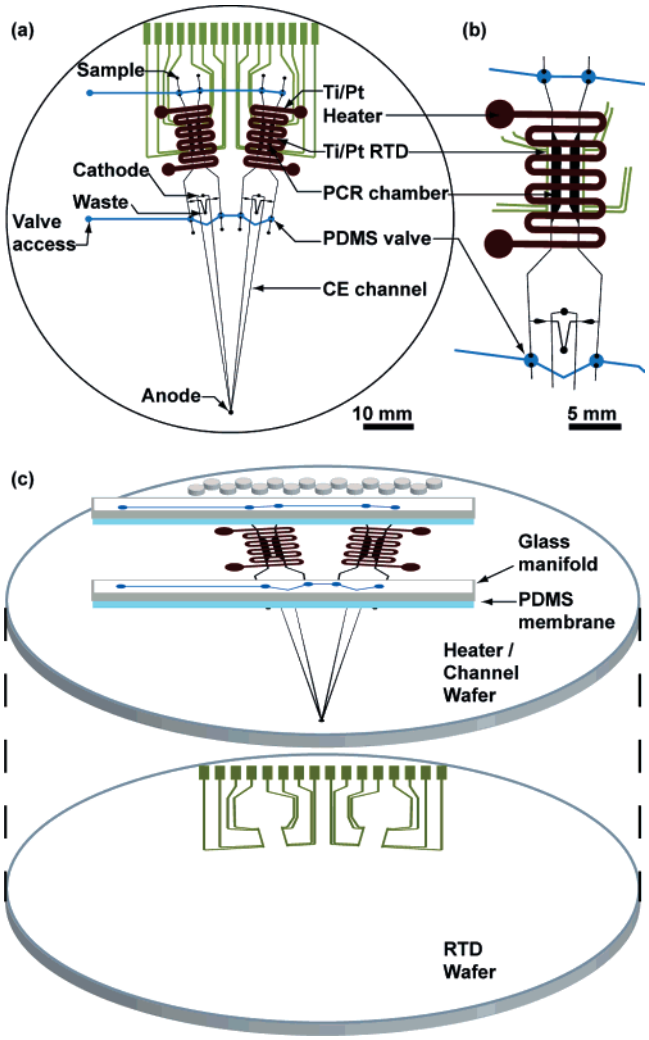

Figure 1. Multichannel PCR-CE microdevice for genetic analysis. (a) The microdevice contains two symmetrical PCR-CE doublets for four independent reactor−separation systems on a 100-mm circular wafer. Each of the doublets contains a resistive heater (red), Ti/Pt RTDs (green), two reaction chambers, two CE separation lanes, and PDMS microvalves for fluidic control. (b) An expanded view of the microfabricated reactor region, showing the relative position of the etched glass reactors to the Ti/Pt heater and RTDs. (c) The integrated microdevice is a four-layer glass-PDMS hybrid structure. The topmost wafer is a glass manifold for fluidic actuation. The second layer is a flexible PDMS membrane, which forms the pneumatically actuated microvalves. The glass heater/channel wafer contains Ti/Pt resistive heaters on the top side along with glass reaction chambers and CE channels etched on the backside. The bottom glass RTD wafer contains Ti/Pt temperature-sensing elements. The glass heater/channel wafer and the RTD wafer are thermally bonded to form the integrated device.

with the relative positions of the PCR chambers, heaters, and temperature sensing elements is shown in Figure 1b.

The microdevice is composed of a glass pneumatic manifold, PDMS membrane, glass heater/electrophoretic channel wafer, and glass RTD wafer (Figure 1c). The etched glass manifold wafer actuates the PDMS microvalves[25] for fluidic control. Two independently addressable Ti/Pt resistive heaters (top side of the heater/channel wafer) and four RTDs (top side of RTD wafer)

(17) Kopp, M. U.; deMello, A. J.; Manz, A. *Science* **1998**, *280*, 1046−1048.
(18) Hashimoto, M.; Chen, P. C.; Mitchell, M. W.; Nikitopoulos, D. E.; Soper, S. A.; Murphy, M. C. *Lab Chip* **2004**, *4*, 638−645.
(19) Obeid, P. J.; Christopoulos, T. K.; Crabtree, H. J.; Backhouse, C. J. *Anal. Chem.* **2003**, *75*, 288−295.
(20) Koh, C. G.; Tan, W.; Zhao, M. Q.; Ricco, A. J.; Fan, Z. H. *Anal. Chem.* **2003**, *75*, 6379−6379.
(21) Liu, J.; Hansen, C.; Quake, S. R. *Anal. Chem.* **2003**, *75*, 4718−4723.
(22) Roper, M. G.; Easley, C. J.; Landers, J. P. *Anal. Chem.* **2005**, *77*, 3887−3893.
(23) Lagally, E. T.; Emrich, C. A.; Mathies, R. A. *Lab Chip* **2001**, *1*, 102−107.
(24) Lagally, E. T.; Scherer, J. R.; Blazej, R. G.; Toriello, N. M.; Diep, B. A.; Ramchandani, M.; Sensabaugh, G. F.; Riley, L. W.; Mathies, R. A. *Anal. Chem.* **2004**, *76*, 3162−3170.
(25) Grover, W. H.; Skelley, A. M.; Liu, C. N.; Lagally, E. T.; Mathies, R. A. *Sens. Actuators, B* **2003**, *89*, 315−323.

are employed to thermally cycle four reactors simultaneously. Temperature feedback for each heater is achieved by averaging the temperature from the two RTDs directly underneath each heater. Reaction chambers and CE separation channels are etched on the backside of the heater/channel wafer, which is bonded to the RTD wafer to yield an all-glass structure.

Microfabrication. The microdevice is fabricated by exploiting procedures described in detail previously.[23] To form the manifold wafer, 0.55-mm-thick D263 100-mm glass wafer (Schott, Yonkers, NY) is coated with 2000 Å of sputtered amorphous silicon (UHV Sputtering, San Jose, CA). Valve seats and actuation channels are defined by spinning photoresist (Shipley 1818, Marlborough, MA) and photolithographically patterned using a contact aligner (Karl Suss, Waterbury Center, VT). The sacrificial silicon is etched using SF_6 in a parallel-plate reactive ion etching system creating a hard mask for subsequent glass etching (RIE, Plasma Therm, St. Petersburg, FL). The exposed glass channels are etched to a depth of 38 μm with 49% CMOS grade hydrofluoric acid at an etch rate of 38 μm/min. The remaining photoresist and amorphous silicon are then stripped from the wafer using PRS-3000 and SF_6 plasma, respectively. Valve actuation holes are drilled using a rotary drill press, and the drilled wafers are diced into 5 mm $\times$ 5 cm strips. PDMS elastomer valves are formed by activating both sides of the PDMS membrane (254-μm-thick HT-6240, Bisco Silicones, Elk Grove, IL) with an UV ozone cleaner (Jelight Co. Inc., Irvine, CA) for 1.5 min to improve PDMS−glass bonding and then sandwiching the membrane between the manifold and the bonded channel wafers.

To form the heater/channel wafer, a 0.55-mm-thick D263 glass wafer is cleaned with piranha solution (20:1 H_2SO_4/H_2O_2) before sputter deposition with 200 Å of Ti and 2000 Å of Pt (Ti/Pt) on the top side and with 2000 Å of amorphous silicon on the backside by dc magnetron sputtering. Ti/Pt heaters are defined by first spinning on photoresist (Shipley 5740) and photolithographically patterned using a contact aligner. The exposed metal is etched using hot aqua regia (3:1 HCl/HNO_3, 90 °C) to form the resistive heaters. PCR chambers and separation channels are then defined on the backside, and the exposed glass regions are etched to a depth of 38 μm. Electrophoresis reservoirs, RTD access holes, and valve via holes are diamond drilled with a computer-controlled CNC mill.

To form the RTD wafer, a 0.55-mm-thick D263 glass wafer is sputtered coated on the top side with 200 Å of Ti and 2000 Å of Pt. Patterns are photolithographically defined and etched as described for the heater to form the 30-μm-wide temperature detection elements and 300-μm-wide leads. The drilled heater/channel wafer is aligned and thermally bonded to the RTD wafer using a programmable vacuum furnace at 580 °C for 6 h (Centurion VPM, J. M. Ney, Yucaipa, CA).

RTD Calibration. The four-wire Ti/Pt RTDs are calibrated after thermal bonding by submerging the wafers in a water bath while maintaining the contact pads above water level. A constant 4-mA current is applied to the outer set of leads while voltage is sensed through the inner set. Voltage is recorded at 5 °C intervals as a function of temperature from room temperature to 95 °C. The corresponding resistance associated with each temperature is calculated using Ohm's law. The data are fitted to the linear function

$$T = A + B \times R \quad (1)$$

where T is the temperature and R is the resistance. Constants A and B are extracted from the fit and are used for temperature feedback during thermal cycling.[23] Due to film variations and Pt oxidation during thermal bonding, the values of A and B vary by 13 and 31% between devices, respectively (95% confidence intervals, $n = 12$). However, the variability of A and B within a device is 2.1 and 6.2%, respectively (95% confidence intervals, $n = 4$). Also, the linear R^2 fit for each individually calibrated RTD is >0.9999. Due to stringent requirement for precise temperature control during thermal cycling, each RTD element on a single wafer is calibrated independently (Supporting Information Figure S-1).

Instrumentation. Thermal cycling is controlled through a LabVIEW program (National Instruments, Austin, TX) with a proportional/integral/differential module. A constant 4-mA source is used to power the RTDs, and the measured voltage from each RTD is collected and filtered using an active low-pass filter (National Instruments 5B backplane). The DAC output then drives the power output from a 0−30 V power supply (GPS-3030DD, Instek, Chino, CA) for the microfabricated heaters at 10 Hz.

The valves on both sides of the PCR chamber were opened and closed using vacuum or pressure supplied through tubing connected to the glass manifold. Pressure and vacuum were supplied by a small rotary pump (G12/02-8-LC, Thomas, Sheboygan, WI), and two solenoid valves (H010E1, Humphrey, Kalamazoo, MI) controlled by a Labview program through a National Instruments DAQ board (PCI-1200) were used to actuate the PDMS valves.

PCR Amplification and Capillary Electrophoresis. The CE separation matrix is 5% (w/v) linear polyacrylamide (LPA) in 1× Tris TAPS EDTA buffer. To minimize electroosmotic flow, the channels are first coated with 50% dynamic coating diluted with methanol for 1 min (The Gel Co., San Francisco, CA, DEH-100). The gel loading procedure then begins by filling the separation channels with LPA through the common anode reservoir. The chambers are then flushed with deionized (DI) water, followed by acetonitrile to sweep bubbles from the chambers. The chambers are flushed again with DI water before PCR samples are loaded into the chambers. Bubble-free sample loading is consistently achieved with this technique. The PDMS elastomer valves are closed after sample introduction by applying 3 psi of pressure to seal the PCR chambers for sample localization and to prevent evaporation during thermal cycling.

The uniformity and the limit of detection experiments were performed with *pUC19* plasmid template (New England Biolabs, Ipswich, MA). The 25-μL reaction cocktail comprises platinum *Taq* Supermix kit (22 units/mL complexed recombinant *Taq* DNA polymerase with platinum *Taq* antibody, 22 mM Tris-HCl (pH 8.4), 55 mM KCl, 1.65 mM $MgCl_2$, 220 μM dNTPs, and stabilizers) (Invitrogen, Carlsbad, CA), 0.4 μM forward and reverse primers (IDT, Coralville, IA), 0.5 ng/μL BSA, and template ranging from 0 to 200 copies/380 nL of reaction volume. This primer set amplifies a 197-bp FAM-labeled amplicon on the *pUC19* plasmid overlapping the multiple cloning sites on the *lac Z*α gene. The

Table 1. PCR Primer Sequences

genome	sequence	product size (bp)
pUC19 (for)	5′-**FAM**-tgcaaggcgattaagttgg-3′	197
pUC19 (rev)	5′-ggctcgtatgttgtgtggaa-3′	
M13mp18 (for)	5′-**FAM**-tggtcgtgtgactggtgaat-3′	230
M13mp18 (rev)	5′-gagtctgtccatcacgcaaa-3′	
E. coli K12 (for)	5′-**FAM**-acgctgcccgatataacaac-3′	237
E. coli K12 (rev)	5′-agcaatggcgtaaaaattgg-3′	

thermal cycling protocol employed is composed of initial activation of the *Taq* polymerase at 95 °C for 40 s, followed by 30 cycles of 95 °C for 5 s, 52 °C for 20 s, 72 °C for 25 s, and a final extension step for 35 s at 72 °C. According to conductive heat-transfer theory, the time required for the temperature to reach equilibrium in a stationary material is proportional to L^2/α, where L is the characteristic thickness of a given region and α is the thermal diffusivity. For 550-μm D263 glass, the calculated time required to stabilize at temperature is ~0.64 s at 95 °C, 1 order of magnitude faster than the thermal transition rates.

M13mp18 single-stranded template (New England Biolabs) and *Escherichia coli* K12 MG1655 cells (American Type Culture Collection (ATCC), Manassas, VA, 700926) are used for the multiplex and genetic identification experiments. *E. coli* cells transfected with a 3.9-kb PCR 2.1-TOPO vector (Invitrogen) for ampicillin and kanamycin resistance are grown overnight on ampicillin plates. Colonies exhibiting resistance are picked and grown overnight in autoclaved LB medium containing 25 μg of kanamycin. Cultured *E. coli* K12 cells are washed three times with 1× PBS. The PCR mixture is composed of 20 μL of platinum *Taq* Supermix, 1 μL each of 0.5 ng/μL BSA, *M13mp18* primers, *E. coli* K12 primers, *M13mp18* template, and *E. coli* K12 cells. The primer sets shown in Table 1, yield a 230-bp amplicon from the *M13mp18* bacteriophage, and a 237-bp amplicon from the *E. coli* cells specific in the *yaiX* gene.

After thermal cycling, the amplified sample is electrophoretically injected and separated in the CE channels using a cross injection scheme. The three-step separation sequence begins with injection of the sample onto the separation column by applying a 225 V/cm electric field between the sample and waste while maintaining a floated cathode and anode. A separation field strength of 250 V/cm is then applied between the cathode and anode while floating the sample and waste. A back-biasing field of 125 V/cm is applied at the sample and waste for 10 s after the separation field is applied for 3 s and are then floated for the remainder of the separation. The electrophoretically separated FAM-labeled amplicons are detected using laser-induced fluorescence with the Berkeley radial microplate scanner[26] providing simultaneous detection from all four lanes.

After each run, the glass manifolds are removed, the PDMS membrane is replaced, and channels and chambers are piranha cleaned to prevent amplicon carryover contamination.

RESULTS AND DISCUSSION

The four-layer glass−PDMS microdevice shown in Figure 1 contains all the elements necessary to amplify and separate genetic materials from four different samples simultaneously. Heaters are fabricated on the top side of a glass substrate, while reaction chambers and separation channels are etched on the backside of the same substrate to ensure good thermal transfer and uniform heating during thermal cycling. Using a microfabricated ring heater to thermally cycle 12 reactors on a 4-in. glass wafer resulted in nonuniform heating across the wafer due to nonuniform film thickness along the heater and edge effects. As a result, the current design employs two independent heaters to thermally cycle four reactors at the center of the wafer. Temperature sensors are fabricated on the RTD wafer to provide precise and fast temperature feedback for rapid thermal cycling. Thermal simulation was used to select the location of the RTDs relative to the reactor to ensure optimum temperature sampling (data not shown).

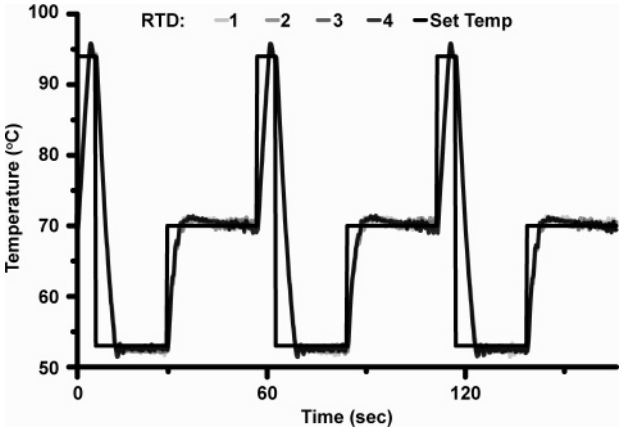

Figure 2. Expanded view of three amplification cycles on the integrated PCR-CE array microdevice. Thermal cycling profiles for all four lanes demonstrate excellent heating and cooling rates and great uniformity across the device (<1 °C/lane). Each cycle of PCR is completed in 50 s (5 s denature, 20 s anneal, 25 s extend). Thirty cycles of PCR amplification are completed in less than 27 min including 40 s of platinum *Taq* activation at 95 °C and 35 s of final extension at 72 °C.

Thermal Cycling. The integrated on-chip resistive heater and temperature detector system demonstrate excellent heating rates and uniformity for rapid thermal cycling (Figure 2). Heating rates exceed 15 °C s^{-1} and active cooling rates are greater than 10 °C s^{-1}, while the interlane temperature difference is <1 °C. Each cycle of PCR is completed in 50 s due to the rapid heating and cooling rates. Thus, 30 cycles of PCR amplification are completed in less than 27 min.

The rate-limiting step for each cycle of PCR is the dwell time at the anneal temperature. With rapid heating and cooling accomplished through integrated on-chip heaters, the burden to further reduce the thermal cycle time has been shifted to the anneal temperature since amplicon length-dependent extension occurs at a rate of 1 kb/min. On-chip optimizations show that a 20-s anneal is the minimum time required for optimal amplification.

Array PCR-CE Microdevice Uniformity. The lane-to-lane variability within the PCR-CE array microdevice was tested with a *pUC19* template. Each of the four reactors is loaded with 200 copies of *pUC19* along with the necessary PCR cocktail and primers. After 30 cycles of PCR amplification, the fluorescently labeled PCR product is electrophoretically injected and separated on the coupled CE channel. A typical PCR-CE array separation

(26) Shi, Y.; Simpson, P. C.; Scherer, J. R.; Wexler, D.; Skibola, C.; Smith, M. T.; Mathies, R. A. *Anal. Chem.* **1999**, *71*, 5354−5361.

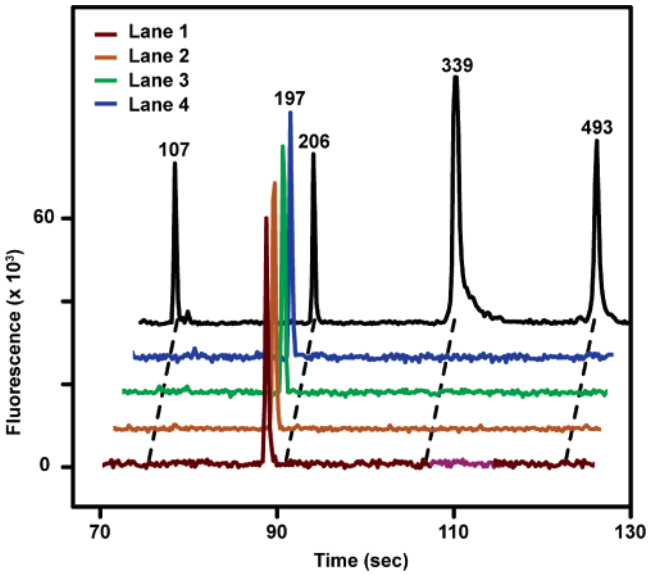

Figure 3. PCR-CE array uniformity study. A *pUC19* plasmid at 200 copies/reaction is thermal cycled 30 cycles and then injected in all four lanes. The expected 197-bp FAM-labeled amplicon is detected in all four reactors. A 107-, 206-, 339-, and 493-bp FAM-labeled ladder injected separately is shown as fragment sizing reference.

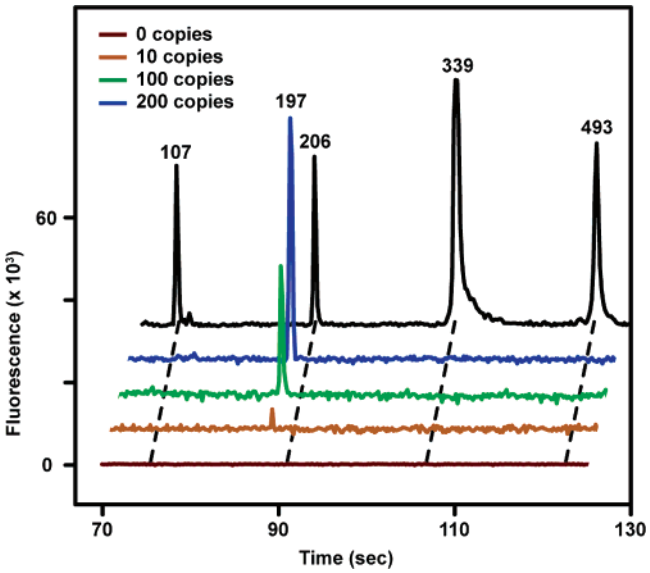

Figure 4. Limit of detection for the integrated PCR-CE array microdevice. A 197-bp amplicon is produced by 30 cycles of PCR from 0, 10, 100, and 200 copies of *pUC19* template ($n = 3$ for each). Electropherogram of the products for the four starting template concentrations is shown (S/N > 10 for the lowest initial copies of 10). Peak heights increase with initial copy number, demonstrating that the reaction is not reactant limited. A 107-, 206-, 339-, and 493-bp FAM-labeled ladder injected separately is shown as fragment sizing reference.

for the 4 lanes with 200 initial copies and 30 cycles of PCR is shown in Figure 3 along with a separately injected FAM-labeled ladder for fragment sizing reference. The microdevice demonstrates good lane-to-lane uniformity with <20 % peak area difference across the four lanes ($n = 12$). The lane-to-lane variability was also evaluated for both 100 and 10 initial copies of *pUC19* template. In both cases, we observed a <30 % peak area difference ($n = 12$). The peak area variation is due primarily to injection

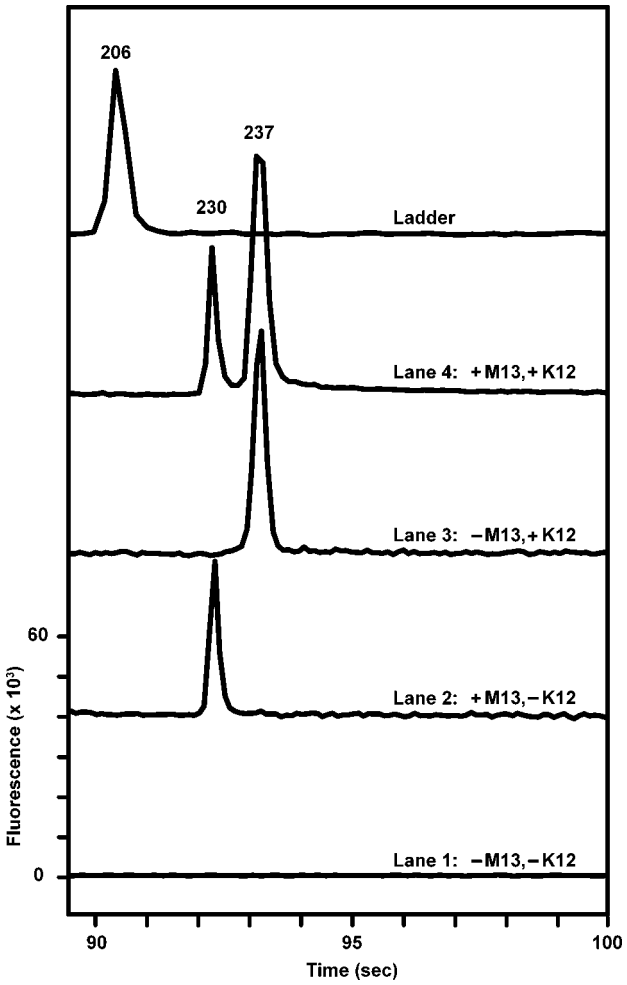

Figure 5. Multiplex PCR analysis of multiple samples in parallel with the PCR-CE array microdevice. Each reaction system is loaded with a different genomic template as follows: Lanes: (1) negative control (0 template molecules), (2) 1000 copies of *M13mp18* plasmid, (3) 1000 *E. coli* K12 cells, and (4) 1000 copies of *M13mp18* plasmid and 1000 *E. coli* K12 cell. All four chambers contain PCR reagents and primer sets for both *M13mp18* (230 bp) and K12 *E. coli* (237 bp) and are thermal cycled 30 times followed by integrated injection and separation.

efficiency differences and irregularities in the gel−sample interface.

Array PCR-CE Microdevice LOD. The LOD for the PCR-CE array microdevice was tested with *pUC19* template by thermal cycling 30 times on-chip and then electrophoretically injecting and separating the amplicons. Electropherograms that resulted from amplifying 200, 100, 10, and 0 initial copies of *pUC19* in the 380-nL reactors are presented in Figure 4. The amplicon peak height still increases with initial copy number after 30 PCR cycles, demonstrating that the amplification is not reactant limited and is still in the exponential regime. The 197-bp peak is detected from just 10 copies (~19 fg of *pUC19* DNA) in the reactor, and the intensity rises strongly at 100 and 200 copies ($n = 3$ for each). The system demonstrates good sensitivity with SN > 10 for 10 initial copies. It should be noted that the negative control (0 initial copies) revealed no production of amplicon, demonstrating that the rigorous piranha cleaning after each array PCR-CE run adequately removes any carryover DNA and does not inhibit future amplifications.

Multiplex Amplification and Genetic Differentiation. The four-lane PCR-CE multichannel microdevice provides a platform for multiplex amplification and genetic detection from four different samples in a single run. The ability to successfully perform multiplex amplification is a good test of thermal cycling characteristics and electrophoretic capabilities because reactors with poor temperature precision and uniformity will produce spurious or low-yield products. In this experiment, the four reactors are loaded as follows: lane 1 with no template (negative control), lane 2 with 1000 copies of *M13mp18* only, lane 3 with 1000 *E. coli* K12 serotype cells only, and lane 4 with both templates (1000 copies of *M13mp18* and 1000 *E. coli* K12 cells). Primers to each genome and PCR supermix are present in all reactors and are thermal cycled 30 times. Figure 5 presents electropherograms for the multiplex array PCR amplification and coupled CE analysis. Lane 1 shows no peaks, indicating the microdevice is free of carryover contamination. Lane 2 shows one peak at 230-bp and lane 3 shows one peak at 237-bp, demonstrating successful genetic amplification and identification of the presence of the *M13mp18* and *E. coli* K12 cells in reactors 2 and 3, respectively. Lane 4 shows two peaks at 230- and 237-bp, corresponding to the successful multiplex amplification from *M13mp18* template and *E. coli* K12 cells. Amplicons separated by 7-bp show full baseline resolution in less than 2 min. The ability to run parallel multiplex PCR makes the multichannel PCR-CE microdevice well suited for high-throughput genetic differentiation assays, as well as applications such as forensic identification and genotyping.

CONCLUSIONS

In summary, a four-lane fully integrated PCR-CE array microdevice has been developed to amplify femtogram (low copy number) amounts of DNA in submicroliter (380 nL) volumes followed by the direct electrophoretic separation of the PCR amplicons, all in <30 min. Integrated heaters and RTDs enable rapid thermal cycling (heating rates of >15 °C s^{-1} and active cooling rates of >10 °C s^{-1}) with interlane temperature variation of <1 °C, resulting in 50 s per PCR cycle and 30 PCR cycles in less than 27 min. The microdevice demonstrates good uniformity across the four lanes and sensitivity down to 10 initial copies with S/N > 10. Multiplex PCR with *M13mp18* and *E. coli* K12 cells illustrates that the microdevice is well-suited for high-throughput genetic differentiation assays.

This microdevice presents a first step toward a scalable PCR-CE platform for improved parallelism. Residual problems that we have identified include glass bonding failure at the integrated heater that leads to bubble generation during sample injection and gel−sample interface irregularities between the PCR chambers and the CE injection channels that lead to peak height variations. Further improvements of the microdevice will include (1) reducing reactor volumes to allow more analysis systems, with reduced reagent volume and faster thermal cycling, (2) a more scalable heater for parallel heating and to alleviate the glass bonding problem, (3) on-chip purification and oligonucleotide−capture of the amplicon[27] to reduce the effect of gel−sample interface injection irregularities, and (4) electronic multiplexing to reduce the number of power supplies required when we transition to a larger number of heaters.

ACKNOWLEDGMENT

We thank Roya Maboudian, Robert Blazej, and Robin Ivestor for their assistance. C.N.L. and N.M.T. were supported by a ChevronTexaco Graduate Fellowship and a NIH Molecular Biophysics Training Grant (T32GM08295), respectively. Microfabrication was performed in the UC Berkeley Microfabrication Laboratory. This work was supported by the NIH under grant R01HG01399 and by the Chemical Sciences Division of the U.S. Department of Energy under contract DE-AC03-76SF00098.

SUPPORTING INFORMATION AVAILABLE

Additional information as noted in text. This material is available free of charge via the Internet at http://pubs.acs.org.

Received for review February 23, 2006. Accepted May 26, 2006.

AC060335K

(27) Paegel, B. M.; Yeung, S. H. I.; Mathies, R. A. *Anal. Chem.* **2002**, *74*, 5092−5098.